Contributions to Entomology 75 (2) 2025, 245–252 | DOI 10.3897/contrib.entomol.75.e154879

CONTRIBUTIONS TO ENTOMOLOGY

SENCKENBERG

Research Article

Treachery pigmentation pattern leads to misidentification: *Tapinoma melanocephalum* (Fabricius), *Tapinoma pygmaeum* (Dufour) and *Tapinoma jandai* sp. nov. (Hymenoptera, Formicidae)

Bernhard Seifert[1]

1 *Senckenberg Museum of Natural History Görlitz, Am Museum 1, D-02826 Görlitz, Germany*

https://zoobank.org/BEE6E96E-8C97-439B-AF57-C63359B41DE5

Corresponding author: Bernhard Seifert (bernhard.seifert@senckenberg.de)

Academic editor: Thomas Schmitt | Received 4 April 2025 | Accepted 13 June 2025 | Published 7 July 2025

Abstract

Discrete color morphs of ants, in the case reported here morphs with whitish versus blackish gaster pigmentation, may be misinterpreted as different species. This became clear in a morphometric study including 91 worker individuals of *Tapinoma jandai* **sp. nov.**, *Tapinoma melanocephalum* (Fabricius, 1793) and *Tapinoma pygmaeum* (Dufour, 1857). The three species are clearly separable by a principal component analysis of 17 morphological characters under exclusion of pigmentation characters. This result is confirmed by a clear separation in a linear discriminant analysis with the classification of any specimen being confirmed with posterior probabilities of $p > 0.9994$. The study showed that just the holotype series of *Tapinoma pithecorum* Seifert, 2022 is a rare color variant of *Tapinoma pygmaeum* and consequently the former taxon is a junior synonym of the latter. In contrast, all remaining samples that formed the basis of the description of *Tapinoma pithecorum* are recognized as an undescribed species which is introduced here as *Tapinoma jandai* **sp. nov.** A consideration of 14 taxa of minute species showing similarities to the new species revealed that none of these is suspected of representing a senior synonym of *T. jandai* **sp. nov.** and that *Tapinoma indicum* Forel, 1895 should be transferred to the genus *Ravavy* Fisher, 2009. Based on examples in *Formica*, *Camponotus*, *Cardiocondyla* and the two cases reported here, it is argued that ant classification by simple color patterns is under increased risk of misclassification.

Key Words

Ant taxonomy, color dimorphism, ghost ant, numeric morphology-based alpha-taxonomy

Introduction

The recent description of *Tapinoma pithecorum* by Seifert, 2022 that was supposed by Seifert (2022) to be a sister species of the notorious pest ant *Tapinoma melanocephalum* (Fabricius, 1793), prompted a phylogenomic investigation of the genus *Tapinoma* Foerster, 1850 with special attention to the relationship of *T. pithecorum* and *T. melanocephalum* (Perez-Flores et al. 2025 accepted). The genetic data confirmed the separate identity of these two species with the last common ancestor dating back 13 million years. The original description of *Tapinoma pithecorum* was based on samples from a greenhouse in Hannover Zoo (holotype series) and of outdoor populations from Pakistan, India, Malaysia, the Fiji and Christmas Islands as well as the south of the Arabian Peninsula (Seifert 2022). The holotype series clustered in a principal component analysis together with the outdoor populations, separating it from *Tapinoma indicum* Forel, 1895 and *T. melanocephalum* (Seifert 2022). However, when making this analysis in 2021, I was not aware of the greenhouse occurrence of *Tapinoma pygmaeum* (Dufour, 1857) and its color dimorphism. This tiny Dolichoderine ant was known until recently only as a native faunal element of the Iberian region, the South of France and Italy. Recent findings in greenhouses of Switzerland

Copyright *Bernhard Seifert*. This is an open access article distributed under the terms of the Creative Commons Attribution License (CC BY 4.0), which permits unrestricted use, distribution, and reproduction in any medium, provided the original author and source are credited.

and Belgium as well as in a domestic garden in England (Seifert et al. 2024) and in urban outdoor habitats near Orleans /France expanded our knowledge on the ecological and geographic range of this species considerably.

These alerting findings prompted a critical reinvestigation of the *Tapinoma pithecorum* material and an extension of sample size under inclusion of *T. pygmaeum*. The unpleasant result was that just the holotype series of *Tapinoma pithecorum* from the greenhouse (but not any other sample I had named *T. pithecorum*) belonged to *T. pygmaeum* when the evaluation excludes gaster pigmentation. The holotype series represents a probably rare case of *Tapinoma pygmaeum* nest population having a whitish gaster being distinctly lighter than the blackish brown head and mesosoma. On the other hand, in structurally and morphometrically clear *Tapinoma melanocephalum* which usually show in dried condition dark heads and mesosomas and whitish gasters, homogenously dark samples occur rarely. I suppose that alternate gaster pigmentation in these related species is directed by a simple mutation and cannot be used as a leading taxonomic character. Since we need a taxonomically available name for the outdoor populations named by Seifert (2022) as *T. pithecorum* and those populations identified genetically by Perez-Flores et al. 2025) as this species, this paper will describe a new species *Tapinoma jandai* sp. nov. and clarify its separation from *T. pygmaeum*.

Material

The backbone of the investigations presented here is Numeric Morphology-Based Alpha-Taxonomy (NUMOBAT, Seifert 2009). Numerically evaluated by direct stereomicroscopic investigation were 25 samples with 51 workers of *Tapinoma melanocephalum*, 8 samples with 17 workers of *T. jandai* sp. nov. and 11 samples with 30 workers of *Tapinoma pygmaeum*. For details see Suppl. material 1.

Methods

Details of equipment, measuring, data analyses and classification procedures are given in Seifert (2022) and Seifert et al. (2024). Principal component analysis (PCA), linear discriminant analysis (LDA), and nested analyses of variance ANOVA tests were performed with the software package SPSS 15.0. In order to give a reader an impression which characters were numerically investigated, character descriptions from these sources are repeated here. Users intending to run their own analyses should study these primary sources. Measuring tiny structures such as basal funiculus segments requires high-resolution stereomicroscopy and careful spatial adjustment. The system used here was a Leica M165C high-performance stereomicroscope equipped with a 2.0× planapochromatic objective (resolution 1050 lines/mm which allowed the use of instrumental magnifications of up to 360×). Sixteen primary measurements were taken in workers (CL, CW, dAN, EL, ExCly, ExClyW, ExOcc, Fu2L, Fu2W, Fu3L, MGr, ML, MW, nExCly, PoOc and SL).

CL Maximum cephalic length measured between points A and B; A is the posteromedian margin point of head capsule; B is an imagined median point situated at the same transversal level as the most anterior points of clypeus left and right of clypeal excision. Bilateral asymmetries are averaged.

CS Cephalic size with CS=(CL +CW)/2.

CW Maximum cephalic width.

dAN Minimum distance of the inner (centripetal) margins of antennal socket rings which is best measurable in dorsofrontal view.

EL Eye length; maximum diameter of the compound eye over all structurally defined ommatidiae; bilateral mean.

ExCly Maximum depth of anteromedian clypeal excision as it appears in frontodorsal view and with median line of head positioned perpendicular in the visual field; bilateral asymmetries are averaged.

ExClyL/W Ratio ExCly /ExClyW.

ExClyW Width of clypeal excision at the level of the base centers of the two most apical and largest setae.

ExOcc Depth of excavation of posterior vertex with head in full face view. Procedure: Using high magnification with low depth of focus, adjust the head to the measuring position defined for CL. Focus both posterior corners of vertex until they form a sharp contour, adjust them to equal horizontal level within the visual field and superimpose the corners with the horizontal line of the cross-scale. Change the focal level until the median part of posterior vertex forms a sharp contour. Read the depth.

Full face view Dorsal aspect of head adjusted for measuring both maximum CL and CW. Use of high magnifications with low depth of focus improve the correct spatial adjustment.

Fu2L Median length of second funiculus segment in dorsal view. Dorsal view is given when the swiveling plane of 1st funiculus segment is positioned in the visual plane. Take care to really measure median length as the segment's sides have unequal length and to recognize the real distal margin of the segment. The latter has a very thin cuticle, frequently producing a narrow, shining ribbon that seems to be, by optical impression, demarcated from the rest of the segment. The median line of the segment is visualized by centre of the patch reflecting the coaxial light.

Fu2W Maximum width of second funiculus segment in dorsal view. Procedure: use the same spatial adjustment of the ant as in measuring Fu2L but rotate it in the visual plane by 90°. The use of transmitted-light is important to visualize the real cuticular surface which is often obscured by pubescence.

Fu3L Median length of third funiculus segment in dorsal view measured under the same conditions as given for Fu2L.

IFu2 Index Fu2L / Fu2W.

ML Mesosoma length from the caudalmost point of lateral metapleuron to rear margin of anterior pronotal fringe (in workers). In workers, if anterior measuring point is concealed, keep the orientation of measuring line, choose a higher magnification, measure from the caudalmost point of lateral metapleuron to the level of promesonotal border and multiply by 1.415. This factor is an average estimated from several species.

MGr Depth of metanotal groove / depression in lateral view; the upper reference line extends between the highest points of mesonotum and propodeum perpendicular to which depth measuring is performed.

MW Maximum pronotal width.

nExCly Bilateral sum of pubescence hairs and smaller setae protruding just visibly at magnifications > 200× across margin of clypeal excision. The two large anteriormost setae are not counted.

PoOc Postocular distance taken in the same spatial adjustment as in measuring CL: distance from the transversal level of posterior eye margin to median point of hind margin of head; bilateral asymmetries are averaged.

SL Scape length excluding articulatory condyle. Transmitted light is useful to visualize the real distal end of scape that may be obscured by pubescence.

Results and discussion

The separation of the three focal species by exploratory and hypothesis-driven data analyses

The separation of *Tapinoma melanocephalum*, *T. pygmaeum* and *T. jandai* sp. nov. was successful on worker individual level without any character selection or the necessity to form nest sample means. A principal component analysis considering all 17 numeric characters given in Table 1 offered a clear separation of three clusters (Fig. 1). The holotype series of *Tapinoma pithecorum* from the greenhouse in Hannover was clearly placed within the cluster of *T. pygmaeum* and is considered as a rare color morph of this species having a whitish gaster. As a consequence, I propose here that *Tapinoma pithecorum* Seifert, 2022 represents a junior synonym of *T. pygmaeum* (Dufour, 1857). On the other hand, two specimens of *Tapinoma melanocephalum* with dark gaster, one from Madagascar and another one from the Solomon Islands, were centrally placed within the cluster formed by the many specimens with a whitish gaster. Apparently, we have here another ant case in which the use of a simple color pattern may lead to misclassification. Similar examples have been reported by Seifert (2018, 2019, 2024) for species of the *Formica rufibarbis* and *Camponotus lateralis* groups and the discrimination of *Cardiocondyla wroughtonii* (Forel, 1890) and *Cardiocondyla obscurior* Wheeler, 1929. In case of conflict between a simple color pattern and complex morphological data, I generally recommend to use the latter. The change of a simple color pattern may be caused by a single mutation (Lus 1932; Barrion and Saxena 1987; Majerus 1998; Andres and Cordero 1999; Majumdar et al. 2008) whereas the change of complex morphologies should require more profound changes in the genome.

In order to assess the probability of the placement of the individuals in the PCA, a character-reduced linear discriminant analysis (LDA) was run using the first four principal components as characters (Fig. 2). Character-reduction was necessary in order to avoid an overfitting of the LDA because the sample size of the smallest class (of *Tapinoma jandai* sp. nov.) consisted of only 17 individuals. The classification of any specimen was confirmed in this approach with posterior probabilities of $p > 0.99$. When run as wild-card, the holotype of *Tapinoma jandai* sp. nov. was classified with $p = 1.000$.

The morphometric data presented in Table 1 indicate that *Tapinoma jandai* sp. nov. shows no difference to *T. pygmaeum* in the majority of characters but is different from *T. melanocephalum* in any character. This might suggest a closer relationship of only the former two species. The index of the second funiculus segment Ifu2 is by far the strongest character to separate *Tapinoma jandai* sp. nov. and *T. pygmaeum* showing no interspecific overlap. Mesosomal width is usually another diagnostic character but the data are compromised by deformation following preparation and drying. Anyway, with the data given in mm, a discriminant

$$539.82*Fu2-41.107*MW-6.910$$

offers a perfect separation with all *Tapinoma jandai* sp. nov. having values < 0 and all *T. pygmaeum* values > 0. A safe separation of *T. jandai* sp. nov. from *T. melanocephalum* is possible by the discriminant

$$80.53*PoOc-74.20*SL+54.56*MW-4.648$$

with all *Tapinoma jandai* sp. nov. having values > 0 and all *T. melanocephalum* values < 0.

Table 1. Morphometric data of three *Tapinoma* species in the sequence arithmetic mean ± standard deviation [minimum, maximum]. The columns with ANOVA data are placed between the columns of the compared species. F values of the strongest differences are given in heavy type.

	***Tapinoma melanocephalum* (i = 51)**	**ANOVA $F_{1,66}$, p**	***Tapinoma jandai* (i = 17)**	**ANOVA $F_{1,45}$, p**	***Tapinoma pygmaeum* (i = 30)**
CS [µm]	438 ± 15 [409, 493]	11.74, 0.001	454 ± 21 [422, 489]	31.80, 0.000	489 ± 20 [443, 517]
CL/CW	1.161 ± 0.027 [1.103, 1.213]	8.17, 0.006	1.141 ± 0.017 [1.107, 1.169]	0.05, n.s.	1.143 ± 0.028 [1.101, 1.218]
SL/CS	0.981 ± 0.023 [0.907, 1.025]	**456.8**, 0.000	0.841 ± 0.023 [0.810, 0.907]	1.02, n.s.	0.847 ± 0.017 [0.815, 0.889]
ExOcc/CS [%]	0.21 ± 0.30 [0.00, 1.39]	8.76, 0.004	0.47 ± 0.37 [0.00, 1.27]	15.72, 0.000	0.98 ± 0.46 [0.08, 2.19]
ExCly/CS [%]	1.51 ± 0.49 [0.64, 2.94]	42.3, 0.000	0.63 ± 0.46 [0.00, 1.66]	0.08, n.s.	0.60 ± 0.29 [0.00, 1.10]
ExClyW/CS [%]	12.66 ± 1.45 [9.80, 15.49]	4.21, 0.044	11.79 ± 1.70 [7.07, 14.60]	0.73, n.s.	11.34 ± 1.71 [8.98, 16.52]
ExClyL/W [%]	0.119 ± 0.036 [0.05, 0.23]	**43.44**, 0.000	0.053 ± 0.035 [0.00, 0.11]	0.01, n.s.	0.054 ± 0.028 [0.000, 0.114]
nExCly	1.88 ± 1.11 [0.0, 5.0]	11.64, 0.001	3.24 ± 2.11 [0.0, 9.0]	28.00, 0.000	0.93 ± 0.86 [0.0, 3.0]
dAN/CS	0.339 ± 0.008 [0.318, 0.358]	33.48, 0.000	0.326 ± 0.009 [0.313, 0.342]	2.33, n.s.	0.323 ± 0.007 [0.304, 0.337]
PoOc/CL	0.469 ± 0.011 [0.434, 0.488]	**57.28**, 0.000	0.495 ± 0.014 [0.461, 0.518]	1.96, n.s.	0.499 ± 0.009 [0.476, 0.511]
EL/CS	0.274 ± 0.010 [0.255, 0.307]	**113.5**, 0.000	0.246 ± 0.008 [0.234, 0.260]	0.58, n.s.	0.245 ± 0.007 [0.230, 0.259]
MGr/CS [%]	2.23 ± 0.80 [1.19, 4.52]	19.21, 0.000	1.31 ± 0.56 [0.20, 2.57]	2.91, n.s.	1.56 ± 0.44 [0.72, 2.47]
MW/CS	0.635 ± 0.018 [0.594, 0.676]	**57.3**, 0.000	0.675 ± 0.022 [0.650, 0.737]	**48.53**, 0.000	0.621 ± 0.027 [0.561, 0.683]
ML/CS	1.240 ± 0.040 [1.119, 1.320]	**69.91**, 0.000	1.152 ± 0.027 [1.094, 1.196]	1.10, n.s.	1.161 ± 0.027 [1.119, 1.228]
Fu2/CS [%]	8.60 ± 0.38 [7.62, 9.35]	**179.3**, 0.000	7.26 ± 0.28 [6.58, 7.65]	**67.32**, 0.000	8.22 ± 0.43 [7.45, 9.10]
Fu3/CS [%]	12.42 ± 0.73 [10.83, 13.77]	**176.0**, 0.000	9.69 ± 0.75 [8.66, 11.42]	0.74, n.s.	9.83 ± 0.37 [9.20, 10.79]
IFu2	0.873 ± 0.046 [0.775, 0.963]	**93.57**, 0.000	0.751 ± 0.040 [0.671, 0.808]	**113.6**, 0.000	0.922 ± 0.059 [0.842, 1.095]

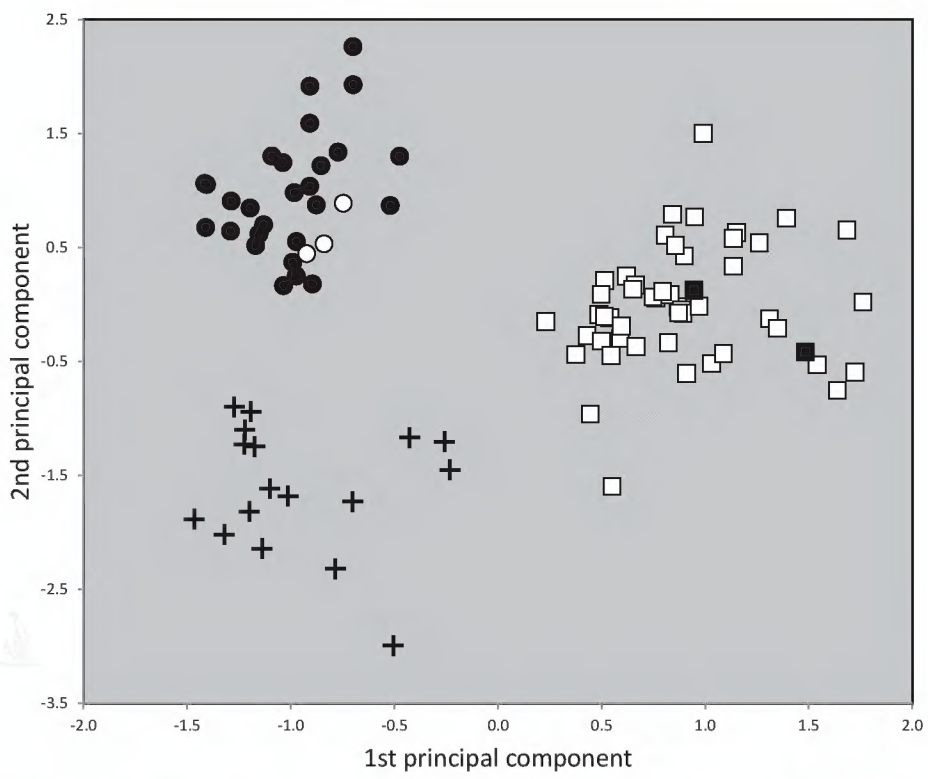

Figure 1. Principal component analysis of worker individuals of three *Tapinoma* species based on 17 morphological characters. *T. jandai* sp. nov. (crosses), *T. pygmaeum* of normal pigmentation (black dots), *T. pygmaeum* with whitish gaster (white dots = the holotype series of *T. pithecorum*), *T. melanocephalum* with whitish gaster (white squares), *T. melanocephalum* with dark gaster (black squares).

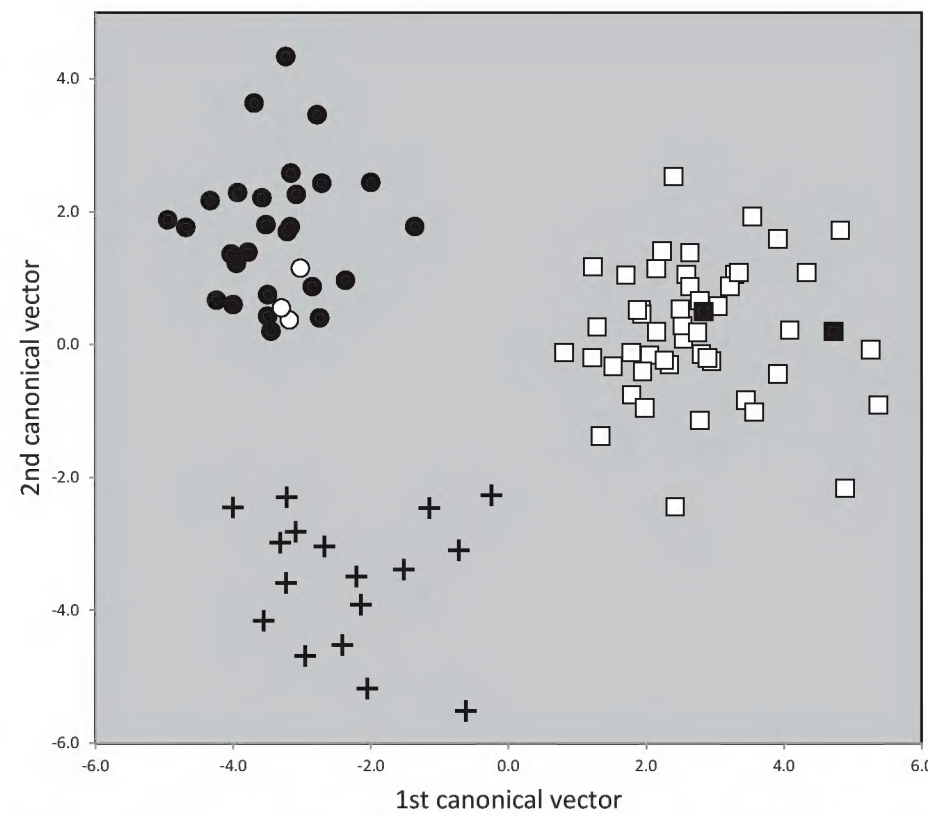

Figure 2. Linear discriminant analysis of worker individuals of three *Tapinoma* species based on four morphological characters. *T. jandai* sp. nov. (crosses), *T. pygmaeum* of normal pigmentation (black dots), *T. pygmaeum* with whitish gaster (white dots = the holotype series of *T. pithecorum*), *T. melanocephalum* with whitish gaster (white squares), *T. melanocephalum* with dark gaster (black squares).

Tapinoma jandai sp. nov.

https://zoobank.org/DFD7F8B8-DF1F-4554-85B2-9BD842308413

Etymology. The name is given in honor of Milan Janda who has collected the holotype specimen and provided valuable other material for this study.

Type material. • Holotype worker labelled "PNG: 5.104°S, 145.775°E, 15 m, Madang: Baitabag, partially fragmented lowland rainforest, M. Janda 2004.01.01-MJ13337" and "Holotype *Tapinoma jandai* Seifert"; • one paratype with the same collecting data label on another pin; • 8 mounted paratype workers on two pins labelled " INDIA: 31.38682°N, 76.47164°E, Himachal Pradesh: Bakhra, 650 m, H. Bharti 2016.05.12 -EX1750"; • 38 paratype workers with identic labelling stored in ethanol; depository SMN Görlitz. The paratype sample coded EX1750 was included in the genomic investigation of Perez-Flores et al. (2025 accepted). For the morphometric

details of all 17 morphometrically examined individuals collected in 8 localities see Suppl. material 1.

Geographic range. Combining the knowledge from this study with two genetically identified samples (Perez-Flores et al. 2025, accepted) which were not available to me, the species is verified for ten sites in the Polynesian and Orientalic Region and the Southeast of the Arab Peninsula. Going from the east to the west, the following picture emerges: Penang / Fiji Islands [-17.364, 178.161, 36 m]; Baitabag / Papua New Guinea [-5.104, 145.775, 15 m]; Koror / Palau Islands [7.34, 134.49, 20 m](sample Ex1730 in Perez-Flores et al. 2025); Christmas Island [-10.48, 105.650, 120 m]; Cameron Highlands-Tana /Malaysia [4.47, 101.37, 1400 m]; Xishuangbanna /China [21.9280, 101.2556, 556 m] (sample Ex1745 in Perez-Flores et al. 2025); Bakhra / Himachal Pradesh [31.38682, 76.47164, 650 m]; Khalghat / Madhya Pradesh [22.16, 75.45, 200 m]; Kagan Valley-Balakot / Pakistan [34.55, 73.35, 1070 m]; Dhofar, Salalah / Oman [17.02, 54.11, 9 m].

Diagnosis. Worker (Figs 3–6; only arithmetic mean of numeric data given here, for full data see Table 1): Minute, mean CS = 454 µm. Head elongated, CL/CW 1.141. Postocular index larger than in *T. melanocephalum*, PoOc/CL 0.495. Hind margin of vertex usually very weakly excavated, ExOcc/CS 0.47%. Anterior clypeal margin not or only very slightly excavated, ExCly/CS 0.63%. Minimum distance of the inner margins of antennal socket rings slightly smaller than in *T. melanocephalum*, dAN/CS 0.326. Scape and 3nd segment of antennal funiculus much shorter than in *T. melanocephalum*, SL/CS 0.841, Fu3/CS 9.69%. Second funiculus segment much shorter than both in *T. melanocephalum* and *T. pygmaeum*, always shorter than wide, Fu2/CS 7.26%, IFu2 0.751 (Fig. 6). Maximum eye diameter notably smaller than in *T. melanocephalum*, EL/CS 0.246. Mesosoma more compact, with a larger width than both in *T. melanocephalum* and *T. pygmaeum*, MW/CS 0.675; longer than in *T. melanocephalum*, ML/CS 1.152. Metanotal depression very shallow, MGr/CS 1.31%. Pubescence hairs on all body surfaces longer and shaggier than in *T. melanocephalum* – as result more fine hairs protruding beyond the anteromedian margin of clypeus, nExCly 3.24. Head and mesosoma medium to blackish brown; gaster, antennae and legs always notably lighter, in dried specimens very pale yellowish or very pale brownish. Accordingly, it shows basically the same light-dark contrasts as usually seen in *T. melanocephalum*. Deviating color morphs not known so far.

Biology. It is a tropical species with basically unknown biology. The holotype sample was collected in a partially fragmented lowland rainforest, the paratype in a dense woodland and the genetically identified sample from China in a tropical botanical garden. The frequency of *Tapinoma jandai* sp. nov. in all collections and all antweb.org images studied is about 10% of that of *T. melanocephalum* and there seems to be no worldwide spreading. This indicates that *Tapinoma jandai* sp. nov. has a much lower tramp species potency than *T. melanocephalum* – if it has any.

Taxonomic comments: exclusion of senior synonymy of other taxa

The large divergence time of 13 My between *Tapinoma jandai* sp. nov. and *T. melanocephalum* estimated by Perez-Flores et al. (2025, accepted) and the many significant morphological differences (see Table 1) indicate that these species are not very closely related. These data exclude that any of the eight taxa synonymized by Guerrero (2018) and Seifert (2022) with *Tapinoma melanocephalum* could be senior synonyms of *T. jandai* sp. nov. As a combination of very short scape and second funiculus segment, wide and short mesosoma, very shallow or absent anteromedian clypeal excavation, large postocular distance and a rather small eye, *Tapinoma jandai* sp. nov. is apparently not to confuse with other tiny congeneric species. This allows identification even by evaluation of z-stack photos. A possible synonymy of *Tapinoma jandai* sp. nov. with the following taxa was checked by evaluation of type specimen images given in https://www.antweb.org and clearly rejected in each case.

Tapinoma minutum Mayr, 1862

The imaged type from Sidney (CASENT0915549) differs by a much longer ratio SL/CL and by the eyes placed more towards the median.

Tapinoma indicum Forel, 1895

The imaged type from Poona (CASENT0909774) has a much shorter head, much broader clypeus and the eyes placed more towards the median. The propodeal profile is not visible in the image but according to head morphology and following the worker diagnosis given by Fisher and Bolton (2016) for the genus it should be transferred to the genus *Ravavy* Fisher, 2009.

Tapinoma fragile Smith, 1876

The imaged type from Mauritius: Rodigues (CASENT0102974) has a much longer scape, much narrower mesosoma and is probably a synonym of *Tapinoma melanocephalum*.

Tapinoma funiculare Santschi, 1928

The imaged type from Tonkin, Yambey (CASENT0911570) differs in having a remarkably oval head in dorsal view and a much longer scape.

Tapinoma atriceps Emery, 1888

The imaged type from Brazil, Rio Grande do Sul (CASENT0904029) has a much longer scape and a narrower mesosoma. The taxon is suspicious to represent a junior synonym of *Tapinoma melanocephalum*.

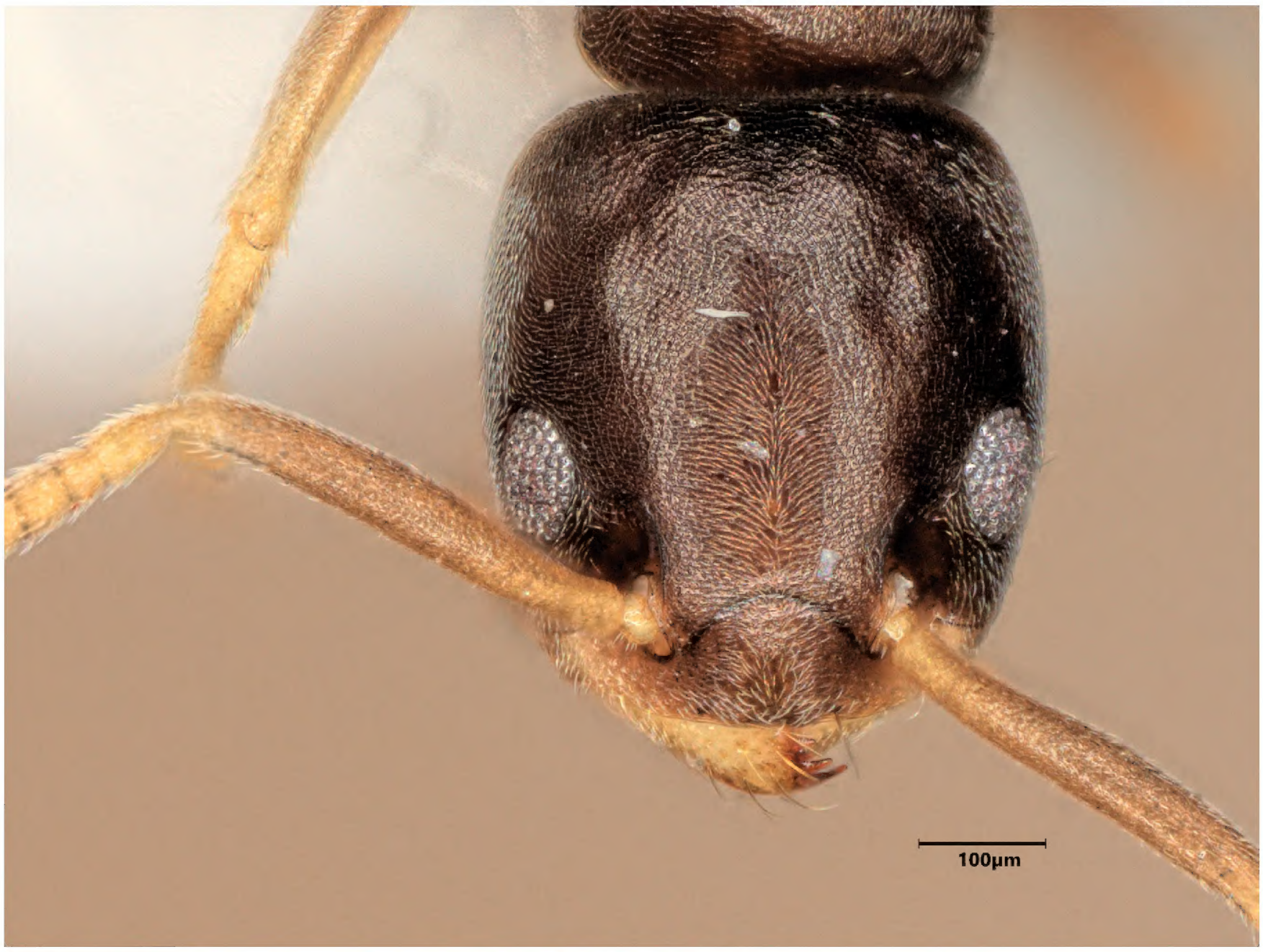

Figure 3. Dorsal aspect of the head of the holotype of *Tapinoma jandai* sp. nov.

Figure 4. Dorsal aspect of the holotype of *Tapinoma jandai* sp. nov.

Figure 5. Lateral aspect of the holotype of *Tapinoma jandai* sp. nov.

Figure 6. Distal scape and basal funiculus segments of the holotype of *Tapinoma jandai* sp. nov. imaged perpendicular to the swiveling plane of the first funiculus segment.

***Tapinoma breviscapum* Forel, 1908**

Two imaged type specimens from São Paulo, Raiz da Serra (CASENT0909768, CASENT0922450) differ radically in the curvature of anterior clypeal margin and in having a much larger absolute size. Head width CW is 499 and 512 µm in the *Tapinoma breviscapum* types whereas it is in *T. jandai* sp. nov. 423 ± 21 [393, 456] µm. Furthermore, the *T. breviscapum* types show a much smaller ratio MW/SL of 0.693 and 0.689 which is in *T. jandai* sp. nov. 0.798 ± 0.025 [0.758, 0.855].

Acknowledgements

I wish to thank Christophe Galkowski, Milan Janda, John Longino, Wouter Dekoninck, Raymond Delarze, Beatrice Viussoz and Brian Fisher for sending collection material. The equipment for the imaging was co-financed by tax money on the basis of the state budget passed by the Sächsischer Landtag according to the Antragsnummer 100590787 of the Sächsische Aufbaubank issued 3 August 2021.

References

Andres JA, Cordero A (1999) The inheritance of female color morphs in the damselfly *Ceriagrion tenellum* (Odonata, Coenagrionidae). Heredity 82: 328–335. https://doi.org/10.1038/sj.hdy.6884930

Barrion AA, Saxena RC (1987) Inheritance of body color in the brown planthopper, *Nilaparvata lugens*. Entomologia Experimentalis et Applicata 43: 267–270. https://doi.org/10.1111/j.1570-7458.1987.tb02220.x

Fisher BL, Bolton B (2016) Ants of the world. Ants of Africa and Madagascar. A guide to the genera. University of California Press, Berkeley, 503 pp. https://doi.org/10.1525/9780520962996

Guerrero RJ (2018) Taxonomic identity of the ghost ant, *Tapinoma melanocephalum* (Fabricius, 1793) (Formicidae: Dolichoderinae). Zootaxa 4410(3): 497–510. https://doi.org/10.11646/Zootaxa.4410.3.4

Lus JJ (1932) An analysis of the dominance phenomenon in the inheritance of the elytra and pronotum color in *Adalia bipunctata*. Trudy Labroratorii Genetiki, Leningrad 9: 135–162.

Majerus M (1998) Melanism: evolution in action. Blackwell, Oxford, UK, 338 pp. https://doi.org/10.1093/oso/9780198549833.001.0001

Majumdar KC, Nasurrudin K, Ravinder K (2008) Pink body color in *Tilapia* shows single gene inheritance. Aquaculture Research 28(8): 581–589. https://doi.org/10.1111/j.1365-2109.1997.tb01078.x

Pérez-Flores O, Branstetter MG, Longino JT, Matos-Maraví P, Borovanska M, Janda M (2025) [accepted] A phylogenomic overview of the ant genus *Tapinoma* Foerster, 1850 (Formicidae: Dolichoderinae), with the phylogeographic history of the ghost ant *Tapinoma melanocephalum*. Insect Systematics and Diversity.

Seifert B (2009) Cryptic species in ants (Hymenoptera: Formicidae) revisited: we need a change in the alphataxonomic approach. Myrmecological News 12: 149–166.

Seifert B (2018) The Ants of Central and North Europe. Lutra Verlags- und Vertriebsgesellschaft, Tauer, 408 pp.

Seifert B (2019) A taxonomic revision of the members of the *Camponotus lateralis* species group (Hymenoptera: Formicidae) from Europe, Asia Minor and Caucasia. Soil Organisms 91(1): 7–32.

Seifert B (2022) The previous concept of the cosmopolitan pest ant *Tapinoma melanocephalum* (Fabricius, 1793) includes two species (Hymenoptera: Formicidae: *Tapinoma*). Osmia 10: 35–44. https://doi.org/10.47446/OSMIA10.4

Seifert B (2024) A taxonomic revision of the ants of the *Cardiocondyla wroughtonii* group (Hymenoptera: Formicidae) with a checklist of the *Cardiocondyla* species of the world. Soil Organisms 96(2): 113–144. https://doi.org/10.25674/415

Seifert B, Kaufmann B, Fraysse L (2024) A taxonomic revision of the Palaearctic species of the ant genus *Tapinoma* Mayr 1861 (Hymenoptera: Formicidae). Zootaxa 5435(1): 1–74. https://doi.org/10.11646/zootaxa.5435.1.1

Supplementary material 1

Coordinates and morphometric data in millimeters

Authors: Bernhard Seifert

Data type: xlsx

Explanation note: Occurrence, morphometric data: primary measurements in millimeters, geographic coordinates and altitude (LAT, LON, ALT).

Copyright notice: This dataset is made available under the Open Database License (http://opendatacommons.org/licenses/odbl/1.0). The Open Database License (ODbL) is a license agreement intended to allow users to freely share, modify, and use this Dataset while maintaining this same freedom for others, provided that the original source and author(s) are credited.

Link: https://doi.org/10.3897/contrib.entomol.75.e154879.suppl1